sciendo

SYSTEM SAFETY: HUMAN - TECHNICAL FACILITY – ENVIRONMENT
7(1), 2025, pp. 375-384

THERMAL ANALYSIS AND TEMPERATURE MONITORING OF A COIL FOR MAGNETIC ORIENTATION OF STEEL FIBERS IN CEMENT COMPOSITES

DOI: 10.2478/czoto-2025-0035
Received: 10/11/2025
Accepted: 14/12/2025

Michał Kordasz[1] – *orcid id: 0000-0003-4193-9244, e-mail: michal.kordasz@polsl.pl*
Maciej Kaźmierowski[2] – *orcid id: 0000-0002-8977-4154, e-mail: maciej.kazmierowski@upwr.edu.pl*
[1]Silesian University of Technology, 44-100 Gliwice, ul. Akademicka 2A, **Poland**
[2]University of Environmental and Life Sciences, 50-375 Wrocław, ul. Norwida 25, **Poland**

Abstract: The study presents an experimental and numerical analysis of temperature variations in a coil used for the magnetic orientation of steel fibers in cement composites. The aim of the research was to assess the thermal safety of the coil during operation and to verify the consistency between experimental measurements and numerical simulations. The test setup consisted of a multilayer coil equipped with seven thermistors placed between the winding layers, enabling real-time temperature recording during a 16-minute power supply and subsequent natural cooling. Numerical analyses were performed in the ANSYS Maxwell environment using a coupled magnetostatic–thermal model that accounted for Joule losses and natural convection. Comparison of the experimental and numerical results showed good agreement (MAE = 1.43°C, MAPE = 3.36%). A nonuniform temperature distribution was observed in the winding, with central layers heating up by approximately 15% more than the outer ones. The results indicate that the analyzed coil, without active cooling, can operate safely only in an intermittent mode. The proposed temperature monitoring method and the regression-based temperature profile description can serve as a basis for the design and thermal optimization of coils used in the magnetic orientation of steel fibers in cement composites.
Keywords: thermal analysis, ANSYS Maxwell, cementitious composites, temperature monitoring, steel fiber orientation

1. INTRODUCTION

One of the methods to improve the tensile strength and crack resistance of brittle cement composites (Szeląg, 2020) is the incorporation of steel fibers into their structure. The presence of fibers allows for partial transfer of tensile stresses after matrix cracking, which limits crack propagation and enhances the deformability of the composite (Domski et al., 2025). The factors determining the interaction of fibers within the matrix – thereby restraining its cracking – include, among others, the fiber content and slenderness, their adhesion to the matrix, and their spatial distribution. Fiber orientation plays a particularly

important role, as alignment with the principal tensile stress directions in the composite enables more effective utilization of their reinforcing potential (Mu et al., 2017).
One promising approach to controlling fiber orientation in fresh cement mixtures is the use of a magnetic field. Steel fibers, being ferromagnetic, can be rotated and aligned parallel to the direction of the magnetic field generated by coils. Previous studies have shown that such alignment can significantly improve the mechanical properties of cement composites, especially in terms of flexural strength and crack resistance (Kaźmierowski et al., 2025).
Various device configurations used for the magnetic alignment of steel fibers in cement composites have been described in the literature. For example, numerous studies employed conventional coils wound with copper wire, into which the mold was placed so that it was located within a region of a nearly uniform magnetic field (Michels and Gams, 2016; Mu et al., 2017; Fernández et al., 2019; Ghailan and Al-Ghalib., 2020; Al Rifai et al., 2024, Kaźmierowski et al., 2025). In such systems, the magnetic field was generated by a copper winding consisting of several dozen turns powered by direct current, and fiber orientation occurred due to the magnetic torque acting on the fibers within the fresh mortar. In another approach, the coil was placed beneath the bottom of the mold so that the magnetic field penetrated upward through the mortar containing steel fibers and fine ferromagnetic particles; this configuration enabled fiber alignment without the need to place the mold inside the coil (Xue et al., 2018). The use of two coaxial coils in a Helmholtz configuration, in turn, allowed for a high degree of magnetic field uniformity within the working space and precise control of magnetic induction (Šonka and Petřík, 2023, Villar and Medina, 2018).
Regardless of the adopted design, a common feature of coils used for fiber orientation is the presence of densely wound copper conductors carrying a high electric current. These parameters determine the magnetic field induction necessary to overcome the viscous resistance of the mixture and to generate a magnetic force capable of rotating the fibers (Mu et al., 2017). However, under prolonged power supply conditions – especially at high current intensity and with limited cooling – the temperature of the windings increases. Excessive heating of the conductors may lead to insulation degradation, reduced coil efficiency, and, in extreme cases, coil failure.
The heating of the winding during current flow results from Joule losses (Gies and Tekkaya., 2017; Karunakaran et al., 2020; Cao et al., 2015). A similar problem occurs in various types of winding such as transformers or electromagnetic coils, as confirmed by different temperature monitoring and control techniques reported in the literature. One of the modern techniques for temperature monitoring is the use of optical fibers. The application of optical fibers enables their deployment in conditions where other solutions may be difficult or even impossible to implement. The literature review highlights their use in fluid-immersed transformers (Cai et al., 2024; Kunicki et al., 2020; Mohammed and Djurović, 2017; Song et al., 2023). However, the major limitation of such systems is the cost of the equipment required for their installation. Consequently, due to budget constraints, this approach may have limited applicability.
Other approaches rely on external temperature measurements such as infrared cameras, laser pyrometers or external thermocouples (Akre et al., 2023) which are ineffective for multilayer coils, while internal measurement techniques are used less frequently. Alongside experimental temperature monitoring, numerical prediction methods (e.g., COMSOL, LS-Dyna) are employed (Gezegin et al., 2021). In parallel, various coil cooling

systems – air- and liquid-based (e.g., using water or oil) – are being developed and optimized to improve heat dissipation efficiency (Konovalov et al., 2023; Lin et al., 2019); however, their application is limited by the need to maintain free airflow between the winding layers.
To date, most studies have focused on the effect of magnetic alignment of fibers, while the issue of the thermal safety of coil operation has been largely overlooked. In this study, a simple method for real – time monitoring of winding temperature using thermistor sensors was proposed, and a thermal analysis was carried out in the ANSYS environment to validate the numerical model. Advanced solutions, such as fiber – optic measurements or active cooling systems, were not considered due to their complexity and cost. The aim of the study was to fill the existing research gap concerning the thermal safety of coils used for the magnetic orientation of steel fibers in cement composites.

2. METHODOLOGY OF RESEARCH

2.1 Objective and assumptions of the experiment

The aim of the study was to investigate the temperature evolution in a coil used for the magnetic orientation of steel fibers in cement composites and to assess the consistency between the experimentally and numerically obtained thermal responses. The magnetic field induction was set to B = 80 mT, which corresponds to the level ensuring effective alignment of fibers within the cement matrix, as confirmed in previous studies (Kaźmierowski et al., 2025). The temperature was measured using thermistors placed between the winding layers during coil operation and after power disconnection, in order to determine the heating and cooling characteristics of the conductors. In parallel, a numerical analysis was performed in the ANSYS Maxwell environment, involving coupled modeling of the magnetic field and heat transfer under conditions corresponding to the actual power supply.

2.2 Test stand

To generate the magnetic field, a coil wound with a copper conductor of 16 mm² cross – section was used. The winding was made on a cylindrical PVC bobbin with a diameter of 150 mm. The coil consisted of 550 turns and was powered by a regulated 8 kW DC power supply, allowing smooth adjustment of current intensity.
To measure the temperature distribution within the winding, seven NTC 3950 thermistors were installed between successive layers of the conductor. An example of the wire winding on the PVC bobbin and the attachment of a thermistor on one of the layers is shown in Fig. 1a, while Fig. 1b illustrates the layout and numbering of the thermistors in the individual winding layers of the coil.

thermistor	layer
t_7	20
t_6	17
t_5	14
t_4	9
t_3	8
t_2	3
t_1	2

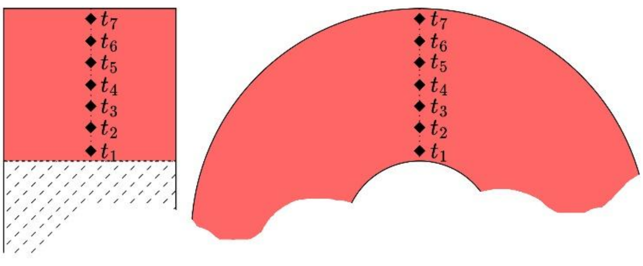

(a) (b)

Fig. 1. (a) Example of wire winding on the PVC bobbin and mounting of a thermistor on one of the winding layers; (b) schematic layout and numbering of thermistors (t_1–t_7) between successive winding layers of the coil

The sensors were calibrated within the temperature range of 20–80°C using a reference resistance thermometer. Signals from the thermistors and the MG – 3002 magnetic field sensor were recorded using an Arduino microcontroller and transmitted to a computer via an RS – 232 interface. The schematic diagram of the experimental setup is shown in Fig. 2.

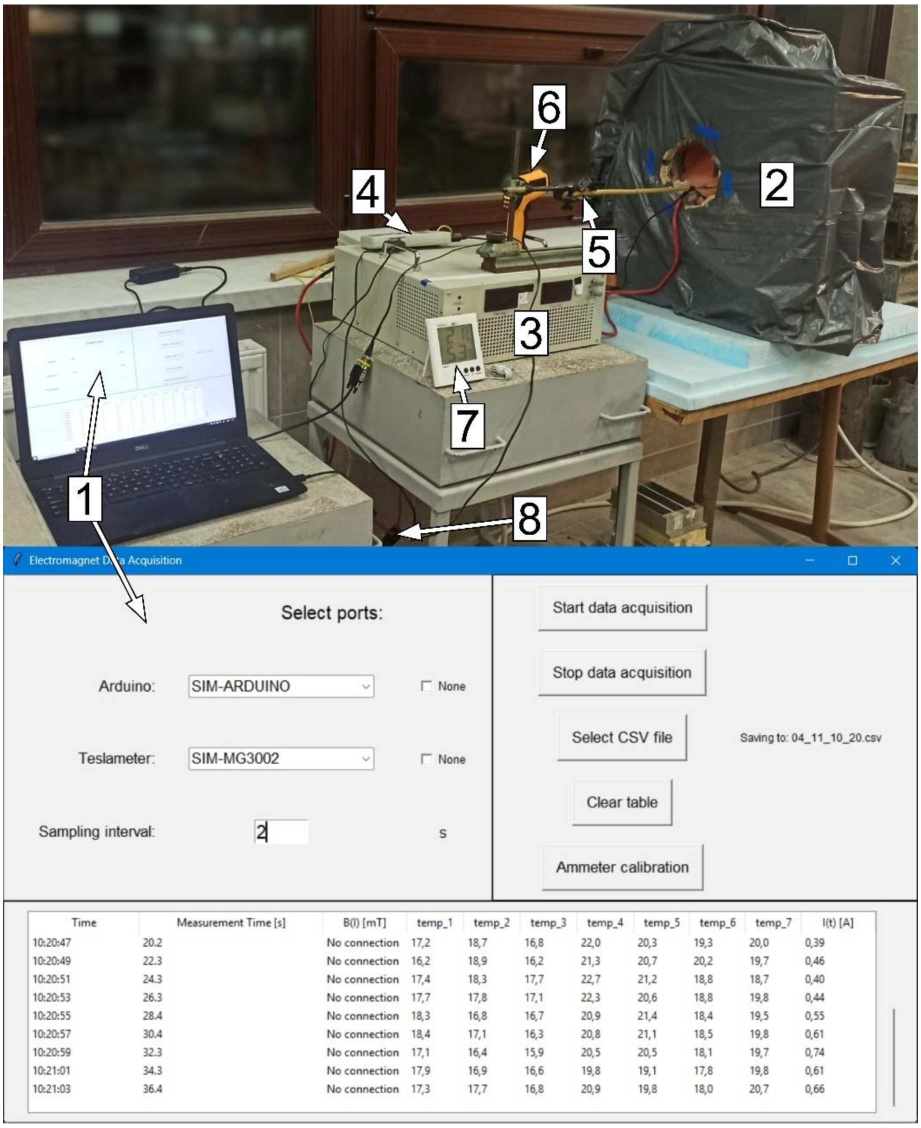

Fig. 2. Experimental setup: 1 – computer with custom data acquisition software (Python); 2 – winding on a PVC bobbin; 3 – DC power supply; 4 – MG – 3002 teslameter; 5 – teslameter probe mounted on a stand; 6 – laser pyrometer; 7 – thermometer and hygrometer; 8 – clamp ammeter

The measurement data – magnetic induction B, temperatures t_1–t_7 from the thermistors, and current intensity I – were recorded in real time using custom software written in Python and equipped with a graphical user interface (GUI). The software enabled data logging in CSV format.

During the tests, the coil was powered with a DC current of 50 A for 16 minutes, after which the power supply was disconnected, and the process of natural cooling by convection was recorded for the next 9 hours and 30 minutes. The air temperature in the laboratory was controlled and maintained at 23 ± 1°C during both the heating and cooling phases. Data were recorded continuously during the power – on period and at 30 – minute intervals after the power was switched off.

2.3 Numerical model and simulation assumptions

The numerical analyses were performed using the ANSYS Maxwell 3D computational environment. The model was developed as a shared framework for the Magnetostatic and Icepak modules, enabling coupled analysis of magnetic and thermal fields. Identical geometry and material properties were applied in both modules, including the copper conductor and the surrounding air domain. The geometry of the coil, along with the current flow direction and current density distribution, is shown in Fig. 3.

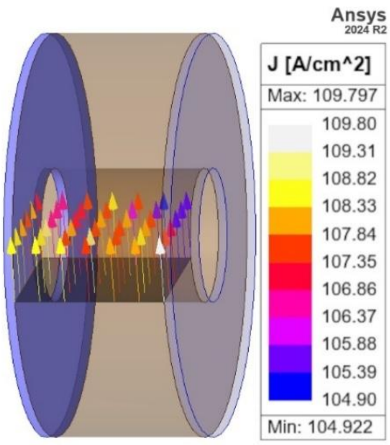

Fig. 3. Three – dimensional model of the coil developed in ANSYS Maxwell. The color scale represents the current density distribution J [A/cm²] in the winding, while the arrows indicate the direction of current flow

In the magnetostatic analysis, the distribution of magnetic induction and current density within the winding was determined, while in the thermal analysis, the Joule effect was considered as the heat source in the conductors, together with heat exchange with the environment through natural convection. The model was constructed using materials available in the program's database (copper, air, PVC), and boundary conditions were defined to replicate the laboratory conditions described in Section 2.2. Simulations were carried out for two coil operating states: Continuous operation, to estimate the maximum temperature that could occur under long – term loading, and 16 – minute operation, corresponding to the actual energizing time in the laboratory experiment.

The limitation of the analysis to these two cases resulted from the adopted research objective, i.e., to determine the characteristic boundary thermal states of the coil without modeling the cooling process, which would require full flow–thermal coupling and significantly increase the computational complexity of the model.

3. RESULTS

3.1 Experimental results

Fig. 4 presents the temperature variations recorded by seven thermistors during the heating and cooling phases of the coil. The points represent the measured values, while the dashed lines correspond to regression functions fitted to the data using the SciPy library (curve_fit function in Python).

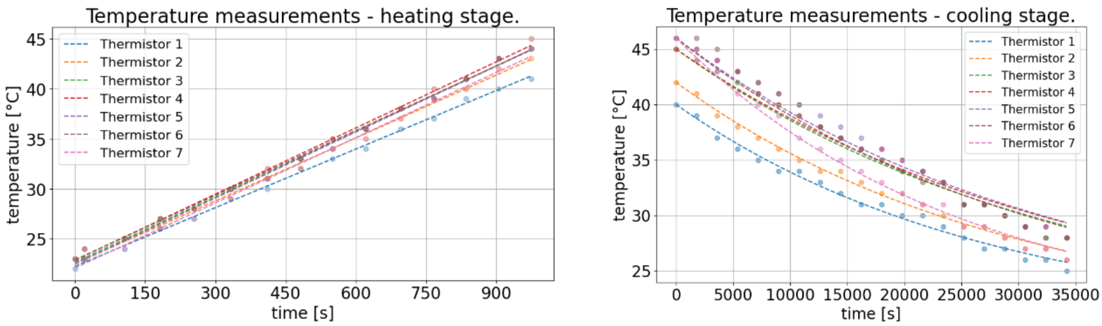

(a) (b)

Fig. 4. Temperature changes in the coil winding recorded by thermistors: (a) during current flow, (b) during cooling after power shutdown. Points represent measured values, while dashed lines indicate fitted regression models – linear (a) and exponential, consistent with Newton's law of cooling (b)

During the current flow period (Fig. 4a), the temperature rise was described by a linear model:

$$T(t) = at + b \tag{1}$$

where a and b are the regression coefficients listed in Table 1. After the power was switched off (Fig. 4b), a gradual temperature decrease was recorded, which was well described by Newton's law of cooling:

$$T(t) = T_{env} + (T_0 - T_{env})e^{-kt} \tag{2}$$

where T_0 i T_{env} denote the initial and ambient temperatures, respectively, and k is the cooling constant. The values presented in Table 1 correspond to the coefficients of the regression equations obtained for the temperatures measured by each thermistor during the heating and cooling phases. In the 'current flow' and 'current – off period' columns, the listed values represent, respectively, the coefficients for Eq. (1) and Eq. (2), as well as the correlation coefficient R^2 (measure of fit) of the regression function with respect to the measured data.

Table 1

Regression coefficients for the heating and cooling stages of the coil

	current flow			**current – off period**	
Thermistor	**a**	**b**	**R^2**	**$k[s^{-1}]$**	**R^2**
1	0,020	22,2	1,00	$3{,}6 \cdot 10^{-5}$	0,97
2	0,021	22,5	1,00	$3{,}4 \cdot 10^{-5}$	1,00
3	0,022	22,6	1,00	$3{,}0 \cdot 10^{-5}$	0,99
4	0,022	22,8	1,00	$2{,}9 \cdot 10^{-5}$	0,98
5	0,022	22,5	1,00	$3{,}0 \cdot 10^{-5}$	0,99
6	0,022	22,9	1,00	$3{,}1 \cdot 10^{-5}$	0,99
7	0,022	22,1	1,00	$4{,}0 \cdot 10^{-5}$	1,00

In the temperature profiles shown in Fig. 4b, clear differences between the individual thermistors can be observed. Their behavior corresponds to the spatial arrangement of the sensors within the winding structure (Fig. 1). Thermistors located in the inner layers (t_1–t_3) recorded lower temperatures compared to those placed closer to the outer surface (t_6–t_7), which results from their limited contact with the surrounding air and lower convection efficiency. The highest temperatures were recorded by thermistor t_7. The differences in temperature evolution confirm the complex nature of heat transfer within the winding, involving radial heat conduction through the copper and surface convection to the surrounding air. The nonuniform temperature distribution also results from variations in current density between layers (Fig. 3), local contact effects, and limited heat exchange caused by the PE film insulation (Fig. 2).

3.2 Numerical results

Fig. 5 presents the numerical simulation results of the coil. Fig. 5a shows the distribution of magnetic induction in the cross – section of the system. The highest field values, reaching approximately 100 mT, occur in the side regions, while in the central part of the coil the induction is close to 80 mT, which is consistent with the assumptions adopted in Section 3.1 and the experimental measurements (Kaźmierowski et al., 2025).

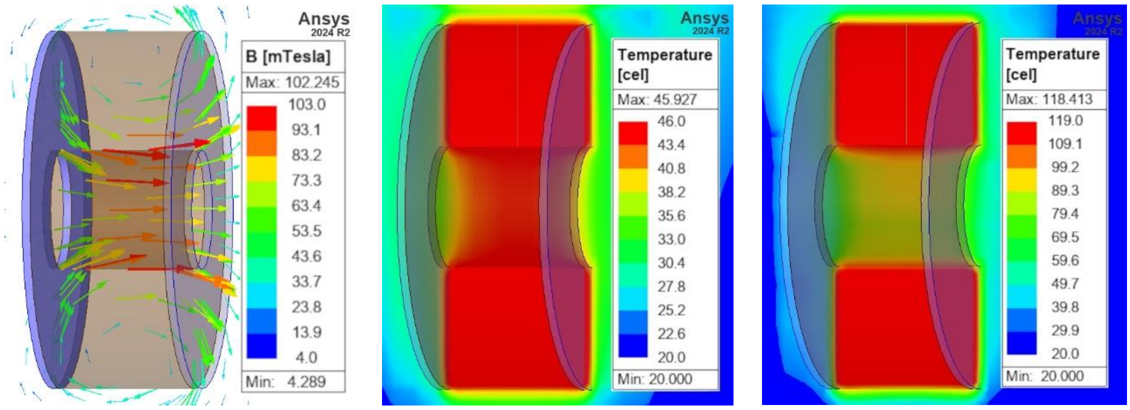

(a) (b) (c)

Fig. 5. Numerical simulation results obtained in the ANSYS Maxwell 3D environment: (a) magnetic induction distribution in the coil with field line directions; (b) temperature distribution in the winding after 16 minutes of operation (conditions corresponding to the experiment); (c) temperature distribution for the continuous operation state of the coil (theoretically infinite power supply duration)

Fig. 5b and 5c illustrate the temperature distribution in the winding after 16 minutes of operation and under continuous operation, corresponding theoretically to an infinite power supply duration. In both cases, an increase in temperature is observed in the central part of the system, whereas the temperature field inside the conductor remains uniform. This results from the geometric simplification adopted in the model, in which the winding was represented as a monolithic copper block with averaged material properties, without distinguishing individual turns or insulation layers. Consequently, the temperature distribution within the conductor volume is uniform, and gradients appear only in the surrounding air. The simulation results indicate that after 16 minutes of operation, the coil temperature does not exceed 50°C, while under continuous operation it reaches values above 100°C. This exceeds the permissible temperature of PVC insulation, confirming the necessity of continuous thermal monitoring during coil operation.

4. DISCUSSION

The comparison between the temperatures obtained from numerical simulations and those measured experimentally refers to the 16 – minute operation period of the coil (Figs. 4a and 5b). The results showed that the differences between numerical and experimental

values fall within the error range of MAE = 1.43°C, MAPE = 3.36%, and RMSE = 1.43°C. The largest deviations were observed for the inner layers (t_1–t_2), where simulated values exceeded the measured ones. These discrepancies may result from the simplified representation of heat conduction in the model and the omission of thermal resistances of the winding insulation and local geometric irregularities. In the outer layers (t_4–t_7), the temperature values obtained from the simulations and measurements were in close agreement.
The temperature distribution analysis revealed a pronounced thermal nonuniformity within the winding. The maximum temperature in the central layers (t_3–t_5) was, on average, 14.7% higher than in the outer layers (e.g., in the second layer), confirming the limited effectiveness of gravitational cooling in the central part of the coil. Consequently, a single – point surface temperature measurement may be subject to significant error and may not reflect the actual thermal state of the coil. Therefore, the use of laser pyrometers or infrared cameras is justified only for coils with a small number of winding layers, whereas multilayer coils require distributed, multi – point temperature monitoring.
The relationship between temperature distribution and cooling conditions is also consistent with findings reported in the literature. It has been shown that active water cooling or forced air circulation can significantly reduce local overheating of the windings and maintain thermal stability even during long – term operation (Carrera et al., 2022). The results of the present study confirm this trend and indicate that the implementation of similar design solutions could improve coil performance without the risk of conductor insulation degradation.
The results indicate that the analyzed coil, with the adopted design and material parameters (a copper conductor with a 16 mm² cross – section and PVC insulation), and without an active cooling system, can operate safely only in an intermittent mode, with breaks allowing the winding temperature to decrease below the permissible level. The maximum continuous operating temperature of PVC insulation is approximately 70–80°C, while values exceeding 100°C may lead to its degradation. In the laboratory tests, the maximum temperature was limited to about 45°C, following the adopted operational safety assumptions to prevent potential damage to the winding. The obtained findings have practical significance for the application of coils in processes involving the magnetic orientation of steel fibers in cement composites. Maintaining a stable magnetic field under controlled winding temperature conditions is essential to achieve a consistent fiber alignment effect, which may be particularly beneficial in concrete prefabricated elements such as beams, slabs, or thin – walled architectural components, where directional fiber anisotropy determines the mechanical performance of the composite. From an industrial perspective, these observations may serve as a reference for the design of laboratory setups and production lines in prefabrication plants utilizing magnetic field – based fiber orientation.

5. CONCLUSION

Based on the obtained measurement results and the conducted analyses, the following conclusions were drawn:

- The temperature distribution within the winding of the air – core coil is nonuniform, and the differences between winding layers indicate the presence of localized zones of increased heating intensity.

- External temperature measurement methods, such as infrared thermography or laser pyrometry, become less effective as the number of winding layers increases.
- The numerical analysis performed in the ANSYS Maxwell environment showed good agreement with the temperature values recorded by thermistors during the 16 – minute operation of the coil.
- The implemented integrated measurement system – comprising a network of thermistors, an Arduino microcontroller, and custom Python – based software – enables effective monitoring of the heating and cooling behavior of the coil. The obtained results may contribute to improving the design and thermal control methods of air – core coils used in the magnetic orientation of steel fibers in cement composites (e.g., in prefabrication plants).
- The developed empirical equations describing the temperature variation over time can be applied under conditions consistent with those presented in this study; however, their applicability beyond this range requires additional verification.

ACKNOWLEDGEMENT

This work was supported by the Wroclaw University of Environmental and Life Sciences (Poland) under the project "POMOST" (grant no N110/0001/22).

REFERENCES

Akre, S., Fofana, I., Yéo, Z., Brettschneider, S., Kung, P., Sékongo, B., 2023. *On the Feasibility of Monitoring Power Transformer's Winding Vibration and Temperature along with Moisture in Oil Using Optical Sensors*, Sensors, 23(4), p. 2310, DOI: 10.3390/s23042310

Al Rifai, M. M., Sikora, K. S., Hadi, M. N. S., 2024. *Magnetic alignment of micro steel fibers embedded in self – compacting concrete*, Construction and Building Materials, 412, 134796, DOI: 10.1016/j.conbuildmat.2023.134796

Cai, C., Wang, J., Wan, L., Wang, C., Yuan, Z., Zhang, J., Lin, H., Shao, J., 2024. *Optical Fiber Composite Winding for In Situ Thermal Monitoring of Transmitter Magnetic Mechanism in Long – Track DWPT Systems*, IEEE Transactions on Instrumentation and Measurement, 73, 1–4, DOI: 10.1109/TIM.2023.3329107

Cao, Q., Han, X., Lai, Z., Xiong, Q., Zhang, X., Chen, Q., Xiao, H., Li, L., 2015. *Analysis and reduction of coil temperature rise in electromagnetic forming*, Journal of Materials Processing Technology 225, 185–194. DOI: 10.1016/j.jmatprotec.2015.02.006

Carrera, K., Künzel, K., Konrád, P., Sovják, R., Papež, V., Mára, M., Fornůsek, J., Kheml, P., 2022. *Concrete lintels reinforced with steel fibres oriented by a magnetic field*. Acta Polytechnica, *62*(5), 531 – 537. DOI: 10.14311/AP.2022.62.053

Domski, J., Laskowska – Bury, J., Dudzińska, A., 2025. *Cracking Behavior of Fiber – Reinforced Concrete Beams Made of Waste Sand*, Applied Sciences, 15(9), 4790, DOI: 10.3390/app15094790

Ferrández, D., Saiz, P., Morón, C., Dorado, M. G., Morón, A., 2019. *Inductive method for the orientation of steel fibers in recycled mortars*, Construction and Building Materials, 222, 243–253, DOI: 10.1016/j.conbuildmat.2019.06.113

Gezegin, C., Ozgonenel, O., Dirik, H., 2021. *A Monitoring Method for Average Winding and Hot – Spot Temperatures of Single – Phase, Oil – Immersed Transformers*, IEEE Transactions on Power Delivery, 36(5), 3196–3203. DOI: 10.1109/TPWRD.2020.3035842

Ghailan, D. B., Al – Ghalib, A. A., 2020. *Magnetic alignment of steel fibres in self – compacting concrete*, Australian Journal of Structural Engineering, 21(1), 333–341, DOI: 10.1080/13287982.2019.1643642

Gies, S., Tekkaya, A.E., 2017. *Analytical prediction of Joule heat losses in electromagnetic forming coils,* Journal of Materials Processing Technology 246, 102–115. DOI: 0.1016/j.jmatprotec.2017.03.008

Karunakaran, P., Osman, M.S., Karuppanna, V., Cheng, S.C., Lee, M.D., Fadhilah, M.D., Lau, A., 2020. *Eddy Current versus Joule Heating Effects for a Cable Suspended in an Iron Pipe*, in: 2020 IEEE International Conference for Innovation in Technology (INOCON). Presented at the 2020 IEEE International Conference for Innovation in Technology (INOCON), 1–6. DOI: 10.1109/INOCON50539.2020.9298438

Kaźmierowski, M., Kadela, M., Kordasz, M., Chyliński, F., Jaskulski, R., Drzazga, M., Wydra, M., Marchwicki, K., Cińcio, A., 2025. *Cementitious Composites Reinforced with Magnetically Oriented Steel Microfibers: Mechanical Properties, Deformability and Fracture Propagation*, Materials, 20(18), 4739, DOI: 10.3390/ma18204739

Konovalov, D., Tolstorebrov, I., Eikevik, T.M., Kobalava, H., Radchenko, M., Hafner, A., Radchenko, A., 2023. *Recent Developments in Cooling Systems and Cooling Management for Electric Motors*, Energies 16, 7006. DOI: 10.3390/en16197006

Kunicki, M., Borucki, S., Zmarzły, D., Frymus, J., 2020. *Data acquisition system for on – line temperature monitoring in power transformers*, Measurement, 161, p. 107909, DOI: 10.1016/j.measurement.2020.107909

Lin, C. – M., Liu, H. – Y., Tseng, K. – Y., Lin, S. – F., 2019. Heating, *Ventilation, and Air Conditioning System Optimization Control Strategy Involving Fan Coil Unit Temperature Control*, Applied Sciences 9, 2391. DOI: 10.3390/app9112391

Michels, J., Gams, M., 2016. *Preliminary study on the influence of fibre orientation in fibre reinforced mortars*, Građevinar, 68(8), 645–655, DOI: 10.14256/JCE.1356.2016

Mohammed, A., Djurović, S., 2017. *FBG Thermal Sensing Features for Hot Spot Monitoring in Random Wound Electric Machine Coils*, IEEE Sensors Journal, 17(10), 3058–3067, DOI: 10.1109/JSEN.2017.2691137

Mu, R., Li, H., Qing, L., Lin, J., Zhao, Q., 2017. *Aligning steel fibers in cement mortar using electromagnetic field*, Construction and Building Materials, 131, 309–316, DOI: 10.1016/j.conbuildmat.2016.11.081

Song, D., Liu, W., Yin, Z., Li, X., Wang, Q., Yan, X., Zhang, X., Wang, F., Qin, Y., Shen, Y., Zhang, Z., Zhao, Y., Cheng, T., 2023. *A temperature sensor based on Er3+/Yb3+ co – doped tellurite fiber for real – time thermal monitoring of transformers*, Ceramics International, 49(17, Part B), 28878–28885, DOI: 10.1016/j.ceramint.2023.06.156

Šonka, Š., Petřík, M., 2023. *Towards Hybrid Fibre Reinforced Concrete Exposed to Electromagnetic Field*, AIP Conference Proceedings, 2780(1), Article 020020, in: Special Concrete and Composites 2021: 18th International Conference, Skalský Dvůr, Czech Republic, AIP Publishing LLC, Melville, NY, DOI: 10.1063/5.0137065.

Szeląg, M., 2020. *Application of an Automated Digital Image – Processing Method for Quantitative Assessment of Cracking Patterns in a Lime Cement Matrix,* Sensors, 20(14), 3859, DOI: 10.3390/s20143859Villar, V.P., Medina, N.F., 2018. *Alignment of hooked – end fibres in matrices with similar rheological behaviour to cementitious composites through homogeneous magnetic fields*, Construction and Building Materials 163(2), 256 – 266, DOI: 10.1016/j.conbuildmat.2017.12.084

Xue, W., Chen, J., Xie, F., Feng, B., 2018. *Orientation of Steel Fibers in Magnetically Driven Concrete and Mortar*, Materials 11(1) 170, DOI: 10.3390/ma11010170